



One-third of global population at cancer risk due to elevated volatile organic compounds levels



Ying Xiong ^{1,2}✉, Ke Du ³ & Yaoxian Huang ¹✉

Outdoor air pollution, particularly volatile organic compounds (VOCs), significantly contributes to the global health burden. Previous analyses of VOC exposure have typically focused on regional and national scales, thereby limiting global health burden assessments. In this study, we utilized a global chemistry-climate model to simulate VOC distributions and estimate related cancer risks from 2000 to 2019. Our findings indicated a 10.2% rise in global VOC emissions during this period, with substantial increases in Sub-Saharan Africa, the Rest of Asia, and China, but decreases in the U.S. and Europe due to reductions in the transportation and residential sectors. Carcinogenic VOCs such as benzene, formaldehyde, and acetaldehyde contributed to a lifetime cancer burden affecting 0.60 [95% confidence interval (95CI): 0.40–0.81] to 0.85 [95CI: 0.56–1.14] million individuals globally. We projected that between 36.4% and 39.7% of the global population was exposed to harmful VOC levels, with the highest exposure rates found in China (82.8–84.3%) and considerably lower exposure in Europe (1.7–5.8%). Open agricultural burning in less-developed regions amplified VOC-induced cancer burdens. Significant disparities in cancer burdens between high-income and low-to-middle-income countries were identified throughout the study period, primarily due to unequal population growth and VOC emissions. These findings underscore health disparities among different income nations and emphasize the persistent need to address the environmental injustice related to air pollution exposure.

Outdoor air pollution poses the greatest environmental health threat, resulting in 4–8 million premature deaths each year^{1–7} due to exposure to fine particulate matter with aerodynamic diameters ≤ 2.5 micrometers (PM_{2.5}) and ozone (O₃). Volatile organic compounds (VOCs), which are key precursors of PM_{2.5} and O₃ pollution, can have significant adverse effects on human health. Acute exposure to VOCs has been linked to an increased risk (0.86–1.25%) of hospitalization for respiratory diseases, such as asthma and chronic obstructive pulmonary disease^{8,9}. Long-term exposure to VOCs has been associated with cardiovascular diseases^{10–12}, neurological disorders¹³, and preterm births¹⁴. Certain VOCs, including benzene and formaldehyde, can pose a lifetime cancer risk via different exposure routes (i.e., inhalation, oral, and dermal) and have been classified as known and probable human carcinogens by the United States Environmental Protection Agency (U.S. EPA)¹⁵, respectively. Based on compelling human and animal evidence, the U.S. EPA estimated that continuous exposure to 1 $\mu\text{g m}^{-3}$ of benzene and formaldehyde in the air over a lifetime would

respectively cause 2.2–7.8 leukemia and 13 lung and nasopharyngeal cancers in a million people¹⁵, with formaldehyde being the highest cancer risk driver among 187 hazardous air pollutants in the US¹⁶.

Numerous studies have focused on measuring ambient concentrations of VOCs and identifying associated health effects at the local, regional, and national scales^{16–24}. For instance, Xiong et al.¹⁹ assessed major VOC sources and corresponding health risks in eight Canadian cities from 2013 to 2018 based on ground observations from the National Air Pollution Surveillance network. They found that the inhalation cancer risk of VOCs in western Canada (7.7×10^{-5}) largely exceeded Health Canada's acceptable risk level, with traffic sites posing the greatest threat to human health, followed by industrial zones, urban centers, and background sites. Strum et al.¹⁶ calculated the cancer risks of 41 hazardous air pollutants collected from over 200 sites across the US and revealed that formaldehyde and benzene comprised most of the cancer risk. They suggested that these estimates were representative of monitoring locations and may not represent population-

¹Department of Civil and Environmental Engineering, Wayne State University, Detroit, MI 48202, USA. ²Department of Climate and Space Sciences and Engineering, University of Michigan, Ann Arbor, MI 48109, USA. ³Department of Mechanical and Manufacturing Engineering, University of Calgary, Calgary, AB T2N 1N4, Canada. ✉e-mail: yingxi@umich.edu; yaoxian.huang@wayne.edu

wide risks. Thus, satellite sensor technologies such as the Ozone Monitoring Instrument (OMI) were necessary for future air toxics measurement and assessment. To overcome the limited coverage of fixed monitoring networks and interferences during VOC sampling, Zhu et al.²⁵ utilized the OMI satellite instrument to map surface formaldehyde concentrations and inferred corresponding cancer risks in the US. They estimated that up to 6600 people in the US would develop cancer due to lifelong exposure to outdoor formaldehyde, despite the OMI-derived formaldehyde concentrations being, on average, 47% lower than those measured at the U.S. EPA ground sites.

To date, there are very few studies evaluating the health risks of VOCs from a global perspective, given temporally and spatially sparse ground monitoring sites (particularly in less developed regions), high cost and complexity of VOC sampling and analysis. One recent study by Partha et al.²⁶ employed a 3-dimensional chemical transport model to simulate global BTEX (i.e., benzene, toluene, ethylbenzene, and xylenes) concentrations and estimated country-level BTEX-induced preterm births in 2015. Considering the significant ($\geq 5\%$) changes in global anthropogenic emissions of non-methane VOC (NMVOC) over the past two decades⁵, our study aimed to address the key knowledge gap by reporting the spatial and temporal variabilities of global surface NMVOC concentrations from 2000 to 2019 through a consistent modeling framework. Additionally, we specifically selected ten NMVOC species (i.e., formaldehyde, acetaldehyde, benzene, toluene, xylenes, propylene, methanol, methyl ethyl ketone, acetonitrile, and hydrogen cyanide), hereinafter referred to as hazardous VOC

(HVOC), from model outputs for health risk assessment based on their toxicity and carcinogenicity (Supplementary Table 1). We estimated lifetime cancer risks associated with inhalation exposure to outdoor carcinogenic VOCs (i.e., benzene, formaldehyde, and acetaldehyde) at regional, national, and global scales, highlighting health exposure disparities across different income nations. Our results are particularly important and significant for less developed regions with limited VOC monitoring networks and a general lack of awareness regarding air pollution, as they provide valuable insights on how to mitigate outdoor VOC pollution and attain health and economic benefits.

Results

Air quality impacts of global NMVOC emissions

The interannual variations of NMVOC emissions from 11 regions and 8 sectors (see Methods) are shown in Fig. 1. Globally, NMVOC emissions have risen from 133.6 Teragrams (Tg) in 2000 to 147.2 Tg in 2019 (Fig. 1d), indicating a relative increase of 10.2% compared to the year 2000. Sub-Saharan Africa (SSA), the Rest of Asia (ROA), and China were predominant emission areas, together contributing to 39.0–50.0% of global annual NMVOC emissions. Compared to significant increases in NMVOC emissions in these regions (by 75.9%, 44.0%, and 21.5%, respectively), the US and Western Europe (WEurope) decreased their NMVOC emissions by 36.4% and 44.8% in 2019 relative to 2000. As a result, the proportions of the US and WEurope in global NMVOC emissions have dropped remarkably, from 12.2% and 7.1% in 2000 to 7.1% and 3.5% in 2019, respectively.

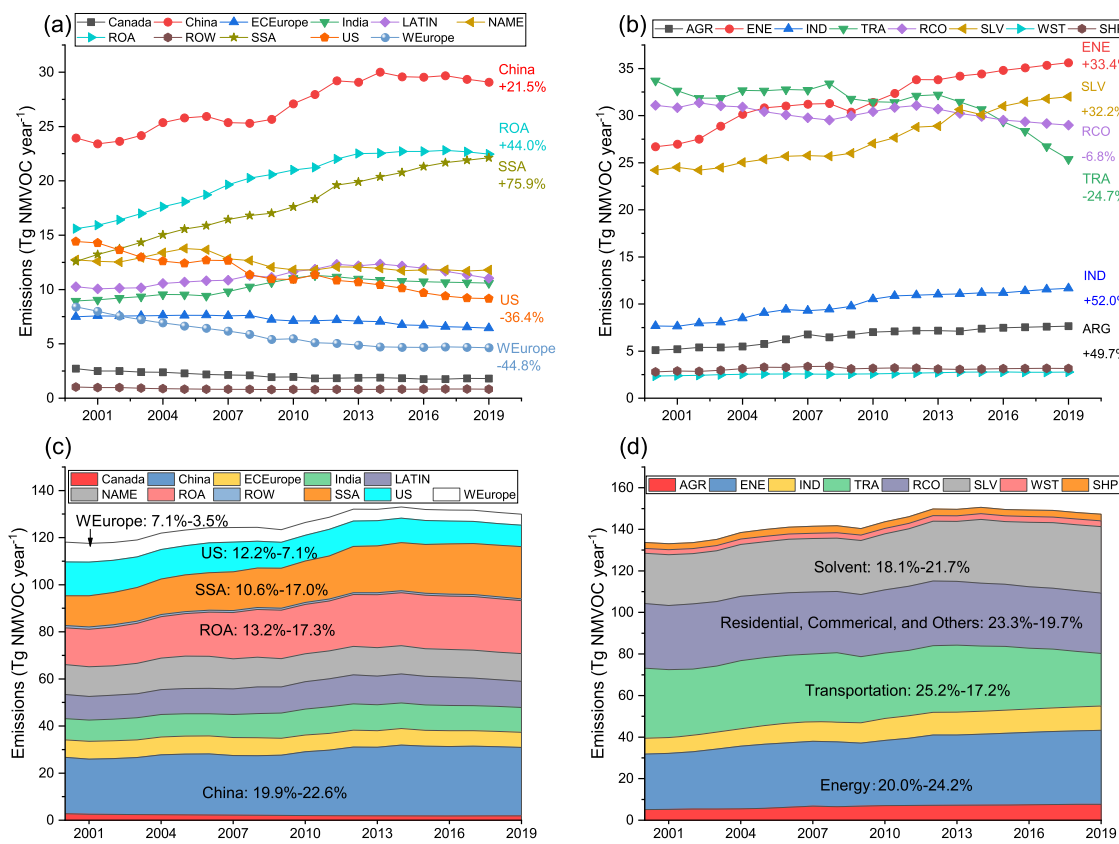


Fig. 1 | Interannual variation of the annual total non-methane VOC (NMVOC) emissions during 2000–2019. a, c NMVOC emissions from 11 regions and b and d are emissions from 8 sectors. The numbers in panels (a, b) represent the relative rate of change in NMVOC emissions during 2000–2019. Percentage values within panels (c, d) indicate the proportions of regional and sectoral emissions in the global annual total emissions for 2000–2019, respectively. The abbreviations used in panels (a, c) are as follows: ECEurope (Eastern and Central Europe), LATIN (Latin America), NAME (Northern Africa and the Middle East), ROA (Rest of Asia), ROW (Rest of the World), SSA (Sub-Saharan Africa), and WEurope (Western Europe). In panels

(b, d), the abbreviations represent the sectors as ARG (agriculture), ENE (energy production), IND (industry), TRA (transportation), RCO (residential, commercial, and other), SLV (solvent), WST (waste), and SHP (international shipping). The global annual total emission of 11 regions in panel (c) is slightly lower than the global total emission of 8 sectors in panel (d), which can be attributed to the contributions of international shipping sector and potential boundary misrepresentation in the country mask file. More details on CEDS sectors can be found in Supplementary Table 2.

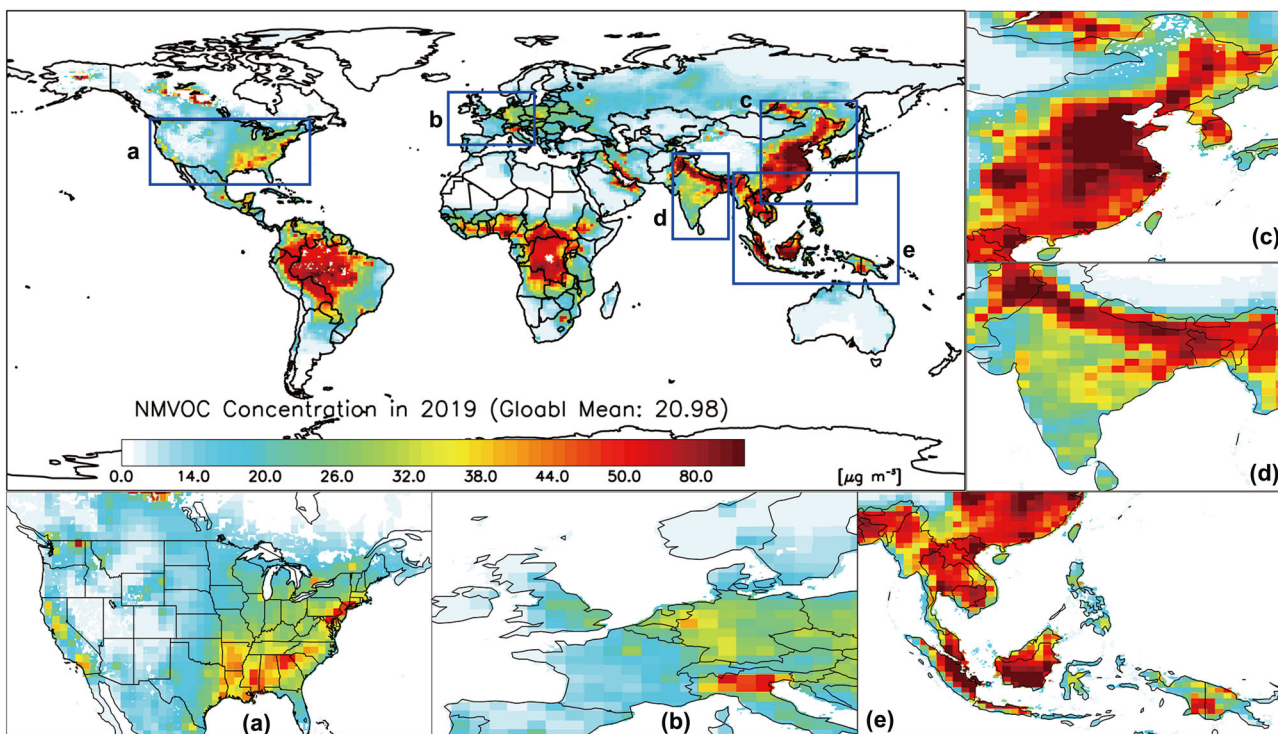


Fig. 2 | Global distribution of population-weighted NMVOC concentration in 2019. The enlarged subplots are **a** the US; **b** Western Europe; **c** Eastern China; **d** India; and **e** Southeastern Asia.

From a sectoral perspective, we found that energy (ENE), solvent usage (SLV), transportation (TRA), residential, commercial, and other (RCO) were the largest four sectors, cumulatively accounting for 82.9%–86.6% of global annual NMVOC emissions during 2000–2019. A clear downward trend has been observed for the transportation (−24.7%) and RCO (−6.8%) sectors, which contrasted with the upward trend of energy (+33.4%) and solvent (+32.2%) sectors (Fig. 1b). The contributions of transportation and RCO sectors to the global annual NMVOC emissions have been overtaken by energy and solvent sectors since 2014 (Fig. 1d). To figure out potential driving factors of emission changes in 11 regions, we additionally analyzed sectoral emissions in each region. As seen in Supplementary Fig. 2, the upward NMVOC emissions in China were dominated by the increases in solvent (+173.3%), industry, and energy emissions, despite remarkable decreases in RCO (−55.0%) and transportation (−48.6%) emissions. The increases in NMVOC emissions in ROA and SSA were driven by the transportation (+66.7%) and energy (+142.6%) sectors, respectively. In contrast, the downward transportation and solvent emissions in the US (−70.8% and −37.5%) and WEurope (−82.7% and −33.5%) were responsible for their decreases in NMVOC emissions during 2000–2019. As for the individual NMVOC, their emission patterns were generally consistent with that of NMVOC. Approximately a third of NMVOC emissions in WEurope, Canada, India, China, Eastern and Central Europe (ECEEurope), and the US were harmful to humans, as inferred by the annual emission ratio of hazardous VOC to NMVOC. Taken together, our findings suggest that despite an upward trend of global NMVOC emissions during 2000–2019, the patterns of emissions varied substantially across 11 regions due to significant differences in economic development and the implementation of regulatory measures. Such differences will likely lead to distinct spatiotemporal distributions of NMVOC concentrations, thus resulting in unequal exposure to hazardous VOC across different income nations.

Figure 2 shows the global distribution of population-weighted NMVOC concentration in 2019. Globally, the annual average concentrations of NMVOC and hazardous VOC respectively increased from 19.3 and 7.8 $\mu\text{g m}^{-3}$ in 2000 to peak levels of 21.2 and 8.8 $\mu\text{g m}^{-3}$ in 2015, before declining slightly to 21.0 and 8.8 $\mu\text{g m}^{-3}$ in 2019 (Supplementary Fig. 3). The

interannual trends in surface NMVOC concentrations were consistent with that of emissions (Fig. 1c). Among the 11 regions, China consistently exhibited the highest NMVOC concentrations, with levels ranging from 35.0 to 41.5 $\mu\text{g m}^{-3}$; this was followed by India (31.8–38.1 $\mu\text{g m}^{-3}$), Latin America (LATIN, 26.6–33.8 $\mu\text{g m}^{-3}$), and ROA (19.5–28.8 $\mu\text{g m}^{-3}$). In contrast, the Rest of World (ROW), Canada, Northern Africa and the Middle East (NAME), and ECEEurope had the lowest NMVOC concentrations, with annual levels unexceptionally lower than 15.0 $\mu\text{g m}^{-3}$ (Fig. 2). We also found that ROA presented the highest percentage increase in NMVOC concentrations (+32.1%) between 2000 and 2019 (Fig. 3a), while WEurope (−43.3%) and the US (−15.6%) showed the largest percentage decreases. Notably, India, China, and LATIN had comparable and the highest hazardous VOC concentrations across all 11 regions throughout the study period (Supplementary Fig. 3).

As for the individual VOC, methanol (CH_3OH) was the most abundant species, accounting for nearly 30% of the total hazardous VOC concentrations, and showed an increasing trend for most regions/countries (Fig. 3f). This trend is consistent with the global increase in industrial and solvent emissions, which are the primary sources of ambient methanol. Formaldehyde (CH_2O), acetaldehyde (CH_3CHO), and methyl ethyl ketone (MEK) also had relatively high concentrations and contributed 34.4–36.0% to the total HVOC. The two carcinogens, CH_2O and CH_3CHO , showed a steady increase in concentrations over ROA, China, India, and Canada, while WEurope and the US displayed an opposite trend from 2000 to 2019 (Fig. 3d, e). Surprisingly, Canada observed a 23.9% and 23.3% increase in formaldehyde and acetaldehyde concentrations, possibly due to secondary atmospheric formations from precursor compounds emitted from the oil and gas operations (e.g., hydraulic fracking, flaring, compression, etc.²⁷) over Alberta's oil sands. This area witnessed 103.9% increase in oil production in 2019 (annual total: 204.5 million m^3) relative to 2007 (the earliest available data, 100.3 million m^3).²⁸ A similar upward trend has been found in other major oil producers worldwide, including Saudi Arabia, Iraq, Iran, Brazil, Nigeria, Venezuela, etc. This suggests that the global increase in oil demand has worsened regional air pollution, which could potentially pose a serious

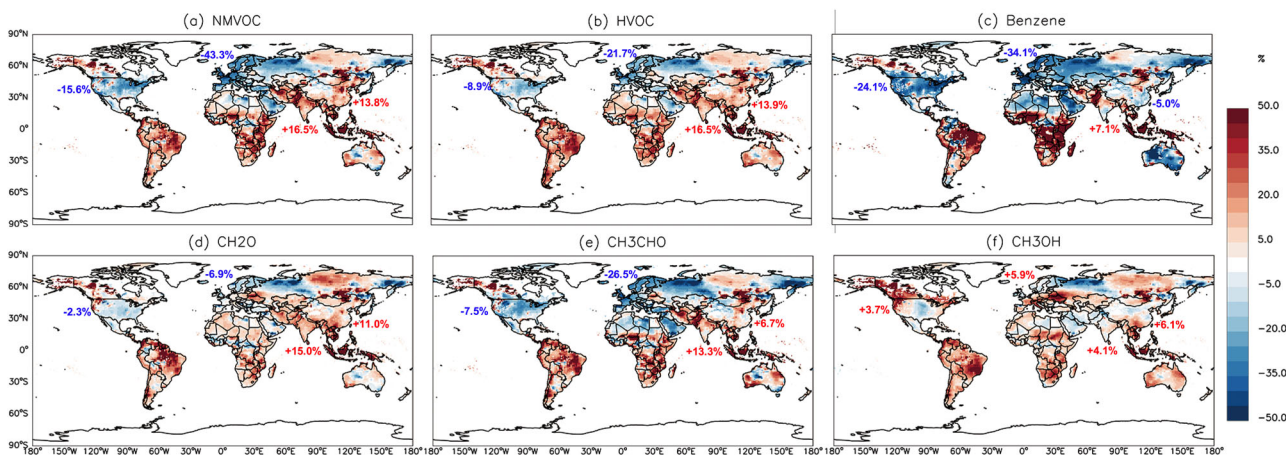


Fig. 3 | Percentage change in surface concentrations of NMVOC during 2000–2019. **a** NMVOC, **b** hazardous VOC (HVOC), **c** benzene, **d** formaldehyde (CH_2O), **e** acetaldehyde (CH_3CHO), and **f** methanol (CH_3OH). The average

percentage changes in the US, Western Europe, China, and India are shown aside, with red and blue colors indicating increase and decrease trends, respectively. The percentage change for the remaining six HVOCs is shown in Supplementary Fig. 4.

threat to human health. Conversely, BTEX was a minor group, with its proportion in the total HVOC declining from 19.5% in 2000 to 17.6% in 2019. Although globally, benzene, toluene, and xylenes showed slight fluctuations (+1.3%, +3.2%, and -0.3%, respectively) over 2000–2019, these fluctuations were not consistent across all regions. Some regions, such as WEurope, the US, and China, have seen significant decreases (by 34.1%, 24.1%, and 5.0%, respectively) in benzene levels (Fig. 3c), while others, such as ROA and SSA, experienced substantial increases (78% and 50%, respectively). The major sources of BTEX, such as solvent use, residential, and transportation sectors, have respectively reduced NMVOC emissions by 37.5%, 61.7%, and 70.8% over the US and 33.5%, 38.9%, and 82.7% in WEurope between 2000 and 2019 (Supplementary Fig. 2). However, these sectors have experienced a 19.1–77.3% increase in NMVOC emissions in ROA and SSA, which explains the inconsistent trend of BTEX concentrations across these regions. In summary, despite the global rise in NMVOC emissions and concentrations from 2000 to 2019, significant variations were still present among the 11 regions. The US and WEurope demonstrated a consistent decrease in NMVOC and hazardous VOC concentrations, opposite to the trend observed in less developed regions such as ROA and SSA.

Health risk of hazardous VOC

The assessment of lifetime inhalation cancer risk (LICR) associated with exposure to benzene, formaldehyde, and acetaldehyde was conducted separately for each age group and then summed up to determine the integrated LICR for 2000–2019. Globally, the integrated LICR showed an increase from 4.2×10^{-5} in 2000 to a peak level of 4.4×10^{-5} in 2015 and 2019 (Fig. 4 and Supplementary Fig. 6). This trend was consistent across all age groups for the three carcinogens. Benzene presented the highest excess lifetime cancer risk, with a global averaged LICR of 2.6×10^{-5} during 2000–2019 (Supplementary Fig. 6). This suggests that, on average, a person exposed to typical benzene levels throughout their lifetime is estimated to have a 26 in a million chance of developing cancer, such as leukemia. Formaldehyde also poses relatively high cancer risks to humans, with an average of 13–14 persons out of a million exposed people developing cancers in their lifetime. Conversely, acetaldehyde showed comparatively low cancer risk, as the global averaged LICRs between 3.1×10^{-6} and 3.5×10^{-6} , representing only 7.5–8.1% of the integrated LICR during 2000–2019 (Supplementary Fig. 6).

Furthermore, we calculated the excess LICR for specific age groups (Supplementary Fig. 7) by considering age differences in sensitivity to carcinogens, intake rate (body weight normalized inhalation rate), and daily activities (fraction of time spent at residential area). The results showed that the 0–2 years old group generally had the highest excess lifetime cancer risks, followed by the 2–9, 9–16, 30–70, 16–30, and third trimester age groups.

This observation is not surprising because a health-protective estimate of cancer risk was employed to account for greater susceptibility in early life, including a 10-fold higher age sensitivity factor and a 3.5-fold higher intake rate (per kg body weight) for 0–2 years old group than those for adults (age 30–70 group, Supplementary Table 7). Consequently, our estimated lifetime inhalation cancer risks, designed for the maximum exposed individual risk to prevent any potential underestimation of impacts on public health, are generally higher than those reported in earlier studies^{21,29–36}. The majority of risks in these earlier studies were not age groups-specific (details can be found in Supplementary Table 9).

The U.S. EPA recommends a range of one-in-a-million (or 1.0×10^{-6}) to one hundred-in-a-million (1.0×10^{-4}) as the “acceptable” lifetime cancer risk, depending on the situation and exposure circumstance³⁷. Health Canada employs 1.0×10^{-5} as its primary risk benchmark for “acceptable” exposure, given the high incidence of cancer in Canada³⁸. Our estimates of global averaged LICR for benzene, formaldehyde, acetaldehyde, and their summation (Supplementary Fig. 6) were generally higher than the lower-bound of the U.S. EPA acceptable level but lower than the upper-bound. However, between 2000 and 2019, a considerable proportion of people worldwide, ranging from 36.4% to 39.7% of the population (Table 1), were exposed to carcinogenic VOC that posed an unacceptably high cancer risk (LICR $> 1.0 \times 10^{-4}$). Approximately 26.3–29.3% of the global population lived in environments that presented an unacceptably high risk of cancer due to exposure to benzene during 2000–2019.

From a regional perspective, there was significant spatial variability in carcinogenic VOCs-induced LICR across 11 regions. Figure 4 shows the global distribution of the integrated LICR associated with exposure to benzene, formaldehyde, and acetaldehyde in 2019. India, China, and ROA were the top three regions with the highest excess lifetime cancer risks (Fig. 4). The integrated LICR in India (1.0×10^{-4} – 1.1×10^{-4}) constantly exceeded the upper-bound of the acceptable risk level set by the U.S. EPA from 2000 to 2019, resulting in a significant proportion of the Indian population (49.4–55.8%, Table 1) being at high risk of contracting cancers during their lifetime. Although the integrated LICR in China (7.9×10^{-5} – 8.7×10^{-5}) was slightly below the threshold risk level, a concerning number of Chinese, ranging from 80.3% to 84.3% of China’s population, were still exposed to unacceptable lifetime cancer risks from exposure to carcinogenic VOCs between 2000 and 2019. Moreover, a significant increase in the exposure populations was also found in the ROA (32.9–47.3%) and SSA (18.6–30.5%) during the 20-year period.

In comparison, the integrated lifetime cancer risks in the US, Canada, and WEurope were respectively 50.1–59.8%, 67.4–70.2%, and 58.5–72.1% lower than that in India (Fig. 4). The proportions of the exposed population were significantly lower in European countries compared to the U.S and

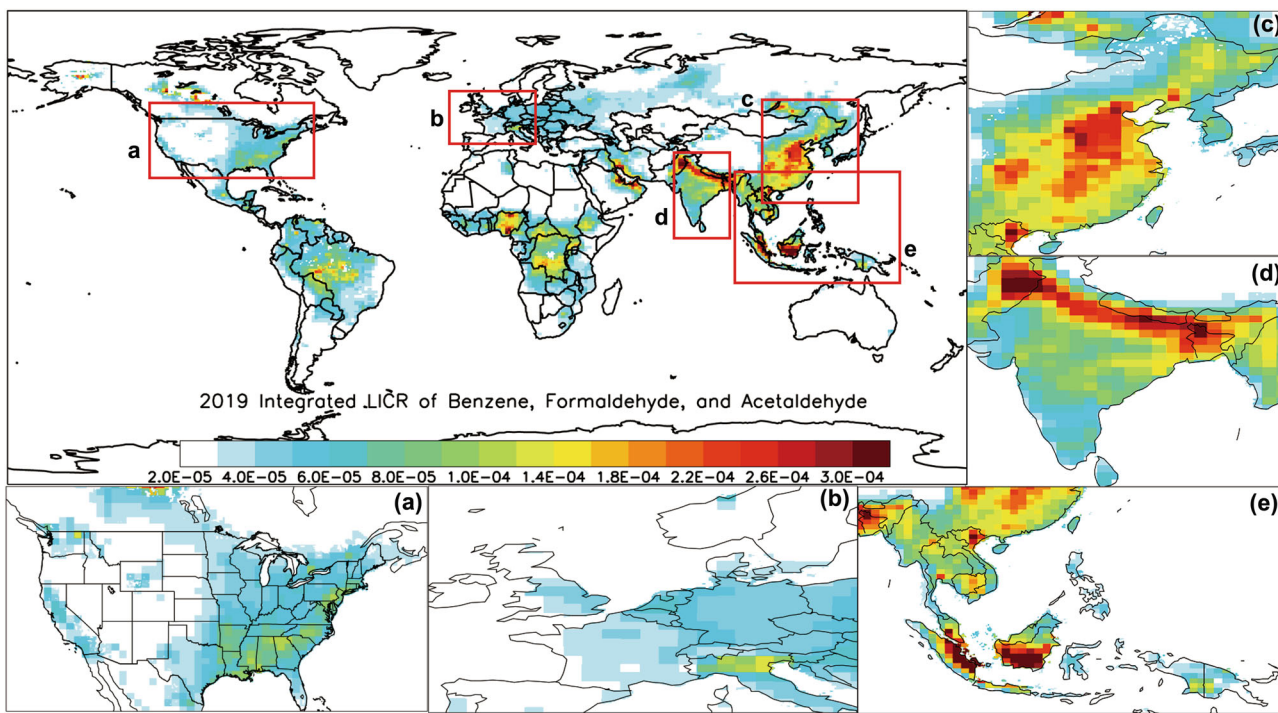


Fig. 4 | Global distribution of the integrated lifetime inhalation cancer risk (LICR) associated with exposure to benzene, formaldehyde, and acetaldehyde in 2019. The enlarged subplots are (a) the US; b Western Europe; c Eastern China; d India; and e Southeastern Asia.

Table 1 | Percentage of regional and global populations exposed to unacceptable levels of lifetime inhalation cancer risk (LICR $> 1.0 \times 10^{-4}$) due to carcinogenic VOCs (comprising benzene, formaldehyde, and acetaldehyde) and benzene (indicated within brackets) from 2000–2019

	2000	2005	2010	2015	2019
China	82.8% (68.2%)	81.4% (65.0%)	80.3% (60.5%)	84.3% (65.5%)	83.2% (64.1%)
India	50.8% (37.8%)	49.9% (40.2%)	54.6% (41.7%)	55.1% (43.6%)	55.8% (44.5%)
ROA	32.9% (22.8%)	38.9% (26.4%)	41.8% (30.9%)	46.2% (36.8%)	47.3% (37.7%)
SSA	18.6% (5.3%)	23.9% (8.6%)	23.3% (13.6%)	28.1% (17.1%)	30.5% (17.6%)
NAME	7.1% (4.8%)	11.7% (5.2%)	11.3% (6.2%)	11.7% (6.6%)	12.6% (6.9%)
LATIN	5.4% (0.2%)	5.9% (0.2%)	5.9% (0.2%)	6.3% (4.1%)	6.3% (0.1%)
ECEurope	2.2% (2.1%)	2.3% (2.2%)	5.8% (2.4%)	2.8% (2.6%)	2.8% (2.7%)
WEurope	3.6% (0.7%)	1.7% (0%)	3.4% (0%)	3.5% (1.1%)	3.5% (0.7%)
US	28.2% (10.8%)	24.3% (8.4%)	13.4% (0%)	9.5% (0%)	4.5% (0%)
Canada	41.2% (30.3%)	36.4% (26.7%)	18.3% (0%)	0.4% (0.1%)	0.4% (0.1%)
ROW	0% (0%)	0% (0%)	0% (0%)	0% (0%)	0% (0%)
Global	36.4% (26.3%)	37.5% (26.7%)	38.0% (26.8%)	39.7% (29.8%)	39.7% (29.3%)

Canada, especially before 2010 (Table 1). Despite a significant decline in the proportions of the exposed population in the US, nearly 4.5% of the population (mostly in the Southeast US, as shown in Fig. 4a) still faced a high risk of developing cancers in 2019. We notably acknowledge the severe impacts of the 2019 Australian bushfires³⁹, which occurred from October 2019 to February 2020, with a peak in December and January. Despite the significant increase in carcinogenic VOCs from these bushfires (Supplementary Fig. 8), the percentage of the population exposed to an unacceptable lifetime risk in the rest of world (ROW) - comprising Australia, New Zealand, and Greenland - remained at 0% in 2019 (Table 1). This is because the LICR, based on the annual mean VOCs, still fell below the threshold for unacceptable lifetime risk (Supplementary Fig. 9). Additionally, the lifetime cancer risk attributable to benzene exposure in Canada (2.4×10^{-5} – 2.6×10^{-5}) was deemed as “unacceptable”, primarily due to substantial emissions from oil sands regions (Supplementary Fig. 10a). A

similar high benzene risk was also found in other major oil-producing regions, particularly in the Middle East. Based on our country-wise estimation, ten countries had a benzene-induced LICRs exceeding the U.S. EPA's upper-bound risk level in 2019. Among them, Bahrain (LICR: 3.7×10^{-4}), Qatar (3.5×10^{-4}), United Arab Emirates (2.3×10^{-4}), and Kuwait (2.0×10^{-4}) had the highest benzene-related cancer risk. Nigeria, the largest oil producer in Africa, also ranked ninth (out of 195 countries) due to its unacceptable high risk (1.1×10^{-4}). Therefore, it is highly recommended to mandate stricter emission control in the oil and gas industry in these countries to reduce primary and secondary emissions of carcinogenic VOCs and protect human health.

In addition to assessing individual risk, we evaluated the population-wide risk by calculating the cancer burden (CB) associated with lifetime exposure to carcinogenic VOCs at global, regional, and national levels. Our analysis revealed that benzene, formaldehyde, and

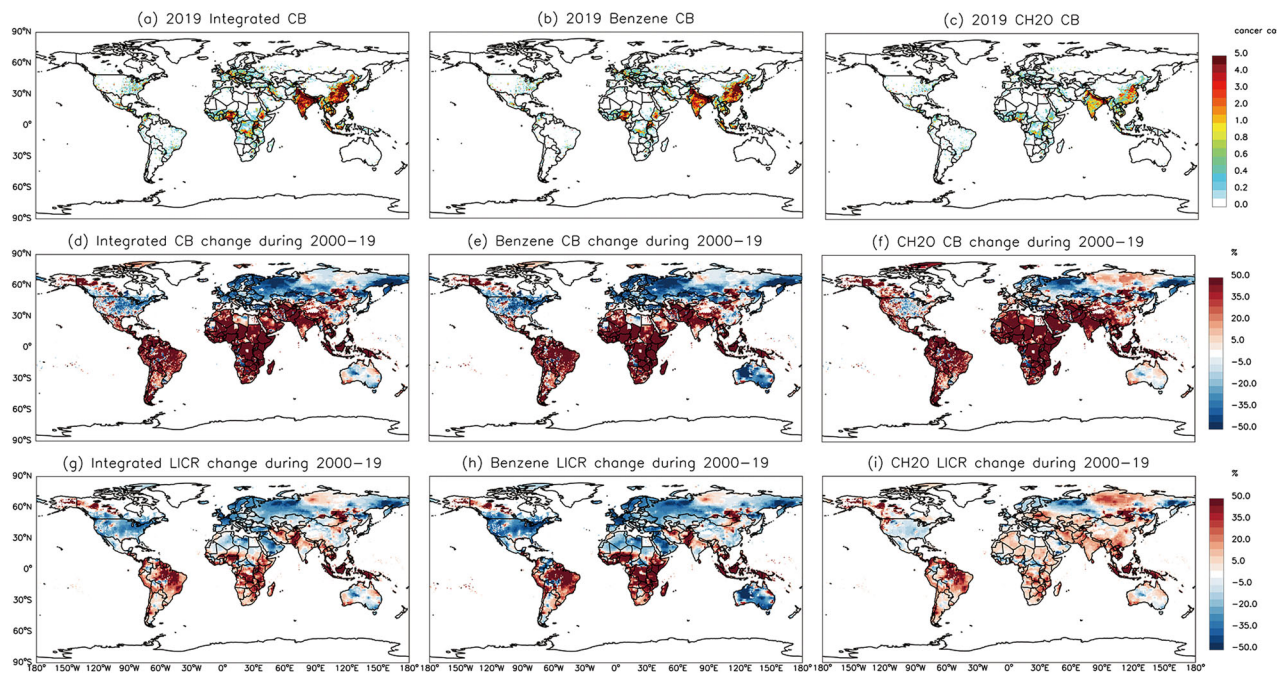


Fig. 5 | Global distribution of total cancer burden (CB) attributable to lifetime exposure to NMVOC. **a** Integrated carcinogens, **b** benzene, and **c** formaldehyde (CH_2O) in 2019. **d–f**, **g–i** represent percentage changes of CB and lifetime inhalation

cancer risk (LICR) for integrated carcinogens, benzene, and CH_2O from 2000 to 2019, respectively. Note that the “during 2000–19” in the subtitle of (d–i) refers to the period from 2000 to 2019.

acetaldehyde exposures were responsible for global total cancer burdens of 0.60 (95% confidence interval (95CI): 0.40–0.81), 0.64 (95 CI: 0.42–0.86), 0.69 (95 CI: 0.46–0.93), 0.79 (95 CI: 0.52–1.06), and 0.85 (95 CI: 0.56–1.14) million for the years of 2000, 2005, 2010, 2015, and 2019, respectively. Benzene exposure contributed to 72.2–74.1% of the integrated cancer burden between 2000 and 2019, followed by formaldehyde (20.5–22.0%) and acetaldehyde (5.4–5.8%). China, India, ROA, and SSA had significantly high cancer burdens (Fig. 5a–c), accounting for 80.8–84.4% of the global annual total during 2000–2019. In contrast, the US and WEurope contributed only 3.9–2.3% and 3.8–2.1% to the global annual total cancer burdens, respectively.

We also ranked countries based on their total cancer burden estimates in 2000, 2015, and 2019 (Fig. 6). The top two countries with the largest population, China and India, represented the highest cancer burdens worldwide due to their high cancer risks. The US respectively ranked seventh and fifth for the total- and formaldehyde-induced CBs in 2019, despite a decrease in LICRs between 2000 and 2019 (Fig. 5g–i). Compared to benzene (Supplementary Fig. 11), the formaldehyde-related cancer burden changed much slower over the US due to a slight decrease in formaldehyde levels (−2.3%, Fig. 3d) in the past two decades. Southern Asian countries such as Indonesia (from 7th in 2000 to 4th in 2019) and Pakistan (from 4th to 3rd), Sub-Saharan African countries such as Nigeria (from 6th to 5th) and the Democratic Republic of the Congo (from 19th to 9th) and Brazil (from 12th to 10th) witnessed an increase in their country rank for the annual total cancer burden. The reasons for the increased rank varied for each country. Severe forest fires in Indonesia in 2015 and 2019 elevated regional benzene (Fig. 3c) and formaldehyde (Fig. 3d) levels and the corresponding cancer burdens (Fig. 5e, f). The Democratic Republic of the Congo, the primary basin of the world’s second largest rainforest (the Congolese), experienced a significant increase in formaldehyde-induced cancer burden (Fig. 6) due to both ‘slash-and-burn’ agricultural practices⁴⁰ – whereby vegetation is cut down and burned before crop planting to enrich the soil – and biogenic emissions. All 195 countries’ estimates of the lifelong cancer burdens in 2000, 2015, and 2019 are available in Supplementary Tables 3–5.

Discussion

The changes in estimated cancer burden for each country and region are influenced by their corresponding VOC emissions, lifetime cancer risk, and population growth. Figure 5d–i displays the global distribution of relative changes in integrated-, benzene- and formaldehyde-induced CBs and LICRs during 2000–2019. There is an obvious opposite trend observed between high-income and low-to-middle-income countries. Between 2000 and 2019, high-income countries such as the US, Canada, and European countries experienced a decline in the integrated- and benzene-induced cancer burdens by 15.4–21.6% and 18.7–28.7%, respectively. Despite a slightly increased population during the period of 2000–2019 (1.1–25.2%, Fig. 7d), anthropogenic emissions of benzene, formaldehyde, and acetaldehyde in these high-income countries separately reduced 11.4–40.6%, 23.3–37.5%, and 16.8–54.1% (Fig. 7a), resulting in 16.6–34.4%, 2.3–6.8%, and 7.5–26.5% (Fig. 7b) of decreases in the estimated LICRs, respectively. Therefore, reducing emissions played a key role in lowering VOC-related cancer burdens in high-income countries. However, an exception was found for formaldehyde, which led to increased cancer burdens among high-income countries (Fig. 7c). This can be explained by the population growth greatly outweighing LICRs reduction. For instance, the US population increased by 21.0% between 2000 and 2019, while the formaldehyde-induced LICR decreased by only 2.3%, resulting in an overall increase in population-wide cancer burden by 14.4%. Interestingly, the study also found that secondary formation of formaldehyde might be significant over Canadian oil sands regions, given reduced primary emissions (−40.6%, Fig. 7a) but elevated surface concentrations and LICRs (+23.9% and +23.3%, Fig. 7b), especially over Alberta oil sands region. Previous studies reported that precursor compounds emitted from oil and gas operations (e.g., hydraulic fracking, flaring, compression, etc.) could contribute to the secondary formation of formaldehyde^{27,41–43}. Therefore, from an air quality management perspective, it is necessary to jointly control formaldehyde and other VOC emissions in oil sands facilities in Canada.

In contrast, low-middle-income and low-income countries respectively experienced increases in integrated- and benzene-related cancer burdens of 7.9–141.0% and 4.0–166.0%, particularly in the SSA and ROA regions, for the

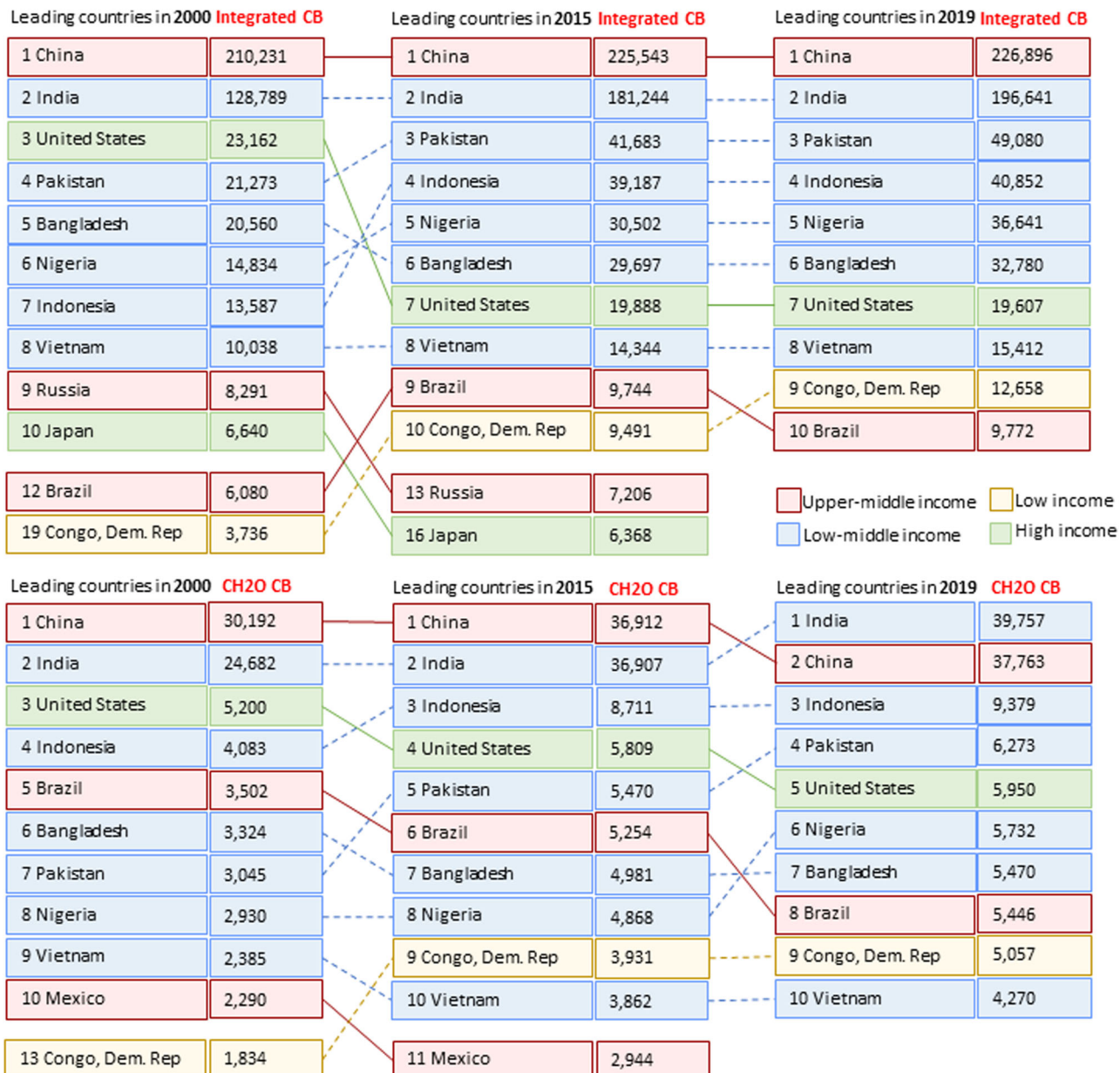


Fig. 6 | Primary countries with the highest integrated- and formaldehyde (CH₂O)-induced cancer burden (CB) in 2000, 2015, and 2019. Income categories are based on the World Bank country classifications for the year 2019.

period of 2000–2019. Sub-Saharan Africa had the fastest growth in population (+79.5%) and VOC emissions (69.4–72.8%, Fig. 7a) during 2000–2019, resulting in the largest increases (98.7–166.0%, Fig. 7c) in population-wide risk in the region. ROA ranked second in terms of relative change in VOC-induced cancer burdens, primarily due to its largest increase in surface VOC concentrations and associated LICRs (39.3–77.8%). China, the country with the highest cancer burden globally (Fig. 6), experienced comparatively small changes (4.2–19.0%). This was primarily because of reduced benzene emissions, which were possibly the result of reductions (−48.6%) in the transportation sector (Supplementary Fig. 2a), and a moderate population growth of 14.2%, during the years of 2000–2019. This trend was also observed in countries within NAME. Given that global population expansion is an unstoppable trend, reducing carcinogenic VOC emissions—particularly benzene—is critical in less developed countries to lower both individual- and population-wide risks in the short term. Moreover, a long-term perspective necessitates proposed strategies to limit formaldehyde emissions in these countries. For developed countries, special attention should be given to the

secondary formation of formaldehyde, as primary emissions of benzene and formaldehyde have substantially decreased over the past two decades.

In this study, we also examined the excess LICR resulting from exposure to VOCs across different economies (low-, low-middle-, upper-middle-, and high-income)⁴⁴ to highlight health exposure disparities. Supplementary Fig. 12 demonstrated that low-middle-income countries have significantly higher exposure risks (up to a factor of 2.1) than low-, upper-middle- and high-income countries. With rapid urbanization and industrialization, low-middle-income countries like India and Nigeria have more complex emission sources of VOC than low-income countries (mostly residential sources and forest fires), making the low-middle-income economies at high cancer risk. We also noticed that low- and low-middle-income countries had much higher risks associated with formaldehyde and acetaldehyde exposure than upper-middle- and high-income countries. This was largely ascribed to wildfires that occurred in these countries, such as the Democratic Republic of the Congo, Indonesia, and the Central African Republic⁴⁰, where slash-and-burn cultivation was

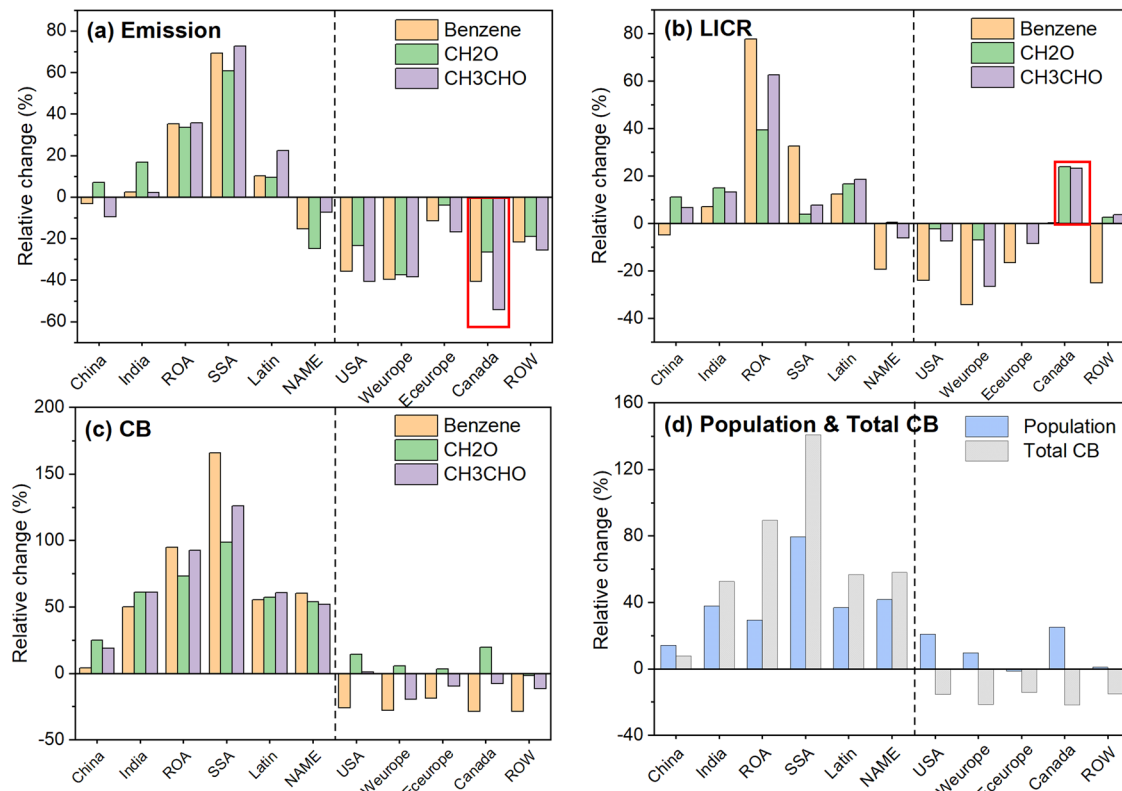


Fig. 7 | The impact of driving factors on estimated cancer burden in 11 regions. Relative changes in **a** anthropogenic emissions, **b** lifetime inhalation cancer risk (LICR), **c** cancer burden (CB), and **d** population in 11 regions between 2000 and

2019. The black dashed line serves to demarcate between high-income countries and those with low-to-middle income.

widely practiced during the agricultural season. Although burning leftover scrub may be fast and economical for farmers, the smoke releases significant amounts of toxic air pollutants (e.g., PM_{2.5}, VOCs), which degrade local and regional (e.g., the 2015 Southeast Asia Haze Crisis) air quality and threaten human health. Given the context of global warming and more frequent heat waves, promoting alternative practices to mitigate open agricultural burning is highly desirable, particularly in low- and low-middle income nations. Between 2000 and 2019, we also observed opposite trends in the VOC-induced lifetime cancer risks between less developed and highly developed economies (Supplementary Fig. 12), which will likely worsen if concrete mitigation strategies are not implemented in low and low-middle-income countries.

Our study has several limitations and assumptions that warrant acknowledgement. Foremost, we assumed the exposures to the mixture of carcinogenic VOCs to be additive. Grounded in our current understanding of these compounds' contributions to cancer risks, we believe this assumption to be reasonable. However, we recognize the complexity of their interactions, which could lead to either synergistic or antagonistic health effects⁴⁵. Second, our risk estimates are based on a limited set of hazardous VOCs, which may not present the total potential cancer risk associated with these pollutants. Out of the 22 VOCs input to the model simulation, we considered 10 VOCs, including three carcinogens, for which the U.S. EPA has dose-response data. We focused on the inhalation exposure pathway and did not consider dermal and ingestion exposures or indoor sources of pollutants (e.g., volatile chemical products from personal care), which might have led to an underestimation of cancer risk. Third, we could not collect exposure variables specific to each country and region, so we assumed the intake rate of each age group to be the same between China and ROA, as well as between the US and WEurope, based on their similar race and physical characteristics. Lastly, there are inherent uncertainties involved in the emission inventory⁴⁶, model configuration⁴⁷, and simulations, which could bias our risk estimates. Although we conducted cross-

validations to test the model's performance in predicting surface VOC concentrations and corresponding cancer risks, caution is needed when interpreting our risk estimates, especially over regions with few ground-based measurements (e.g., SSA, ROA, NAME, etc.). The coarse horizontal model resolution of CAM6-Chem may not be well representative of overall exposure variations in those grid cells with varying landscapes and large concentration gradients. Despite these limitations, our study is distinctive in utilizing a state-of-the-science climate-chemistry model to estimate the individual- and population-wide excess lifetime cancer risks associated with carcinogenic VOC exposure. We provide a comprehensive global view of the unequal spatiotemporal distribution of VOC exposure over the past 20 years, which has significant implications for addressing persistent health exposure disparities among different regions.

In summary, this study utilized the newly developed Community Earth Data System (CEDS) emission inventory and a global chemistry-climate model to analyze spatial and temporal variations of VOC concentrations and shed light on the unequal distribution of global air pollution exposure over the past two decades. Our results showed that an alarming 36.4–39.7% of the global population were exposed to carcinogenic VOC with an unacceptably high cancer risk during 2000–2019. Of particular concern was China, where this proportion remained extremely high (82.8–84.3%) throughout the study period, while it was significantly low in European countries (1.7–5.8%). The US and Canada also witnessed a significant decline in the exposed populations, mainly due to substantial reductions in benzene emissions. In contrast, the low- and low-middle-income countries experienced a consistent increase in VOC emissions between 2000 and 2019, leading to 1.6–2.2-fold higher lifetime excess cancer risks from VOC exposure than high-income countries. Therefore, we propose a different priority mitigation strategy for the low-to-middle-income countries (benzene-based reduction) and high-income countries (secondary formaldehyde-based) to effectively reduce VOC exposure. Our findings are of value for evaluating the long-term health burdens of

global VOC exposure and for addressing the exacerbated health exposure disparities among different income nations.

Methods

Model Simulation

In this study, we utilized a state-of-the-art three-dimensional chemistry-climate model, the Community Earth System Model (CESM version 2.2.0) Community Atmosphere Model with Chemistry, version 6 (CAM6-Chem)⁴⁸, to investigate global trends in surface NMVOC concentrations for the period of 2000–2019 (for model configuration details, refer to Supplementary Table 6). CAM6-Chem model has been widely used to simulate global tropospheric and stratospheric atmospheric composition, given its comprehensive chemistry mechanisms, namely the Model for OZone and Related chemical Tracers – Tropospheric and Stratospheric chemistry (MOZART-TS1)⁴⁷ and the four-mode version of the Modal Aerosol Model⁴⁹. Additionally, secondary organic aerosols in CAM6-Chem are also parameterized via the volatility basis set approach, which has led to an improved response of organic aerosol to emissions and climate change⁵⁰. We ran the CAM6-Chem model at a horizontal resolution of 1.25° in longitude and 0.9° in latitude with specified dynamics using the Modern-Era Retrospective analysis for Research and Applications, version 2 meteorological fields. Each model simulation was run at 5-year intervals from 2000 to 2019, with the first year as a spin-up and the remaining years for results analysis.

The global anthropogenic emission inventory for trace gases and aerosols used in CAM6-Chem model were primarily based on the Community Earth Data System (CEDS) release v2021_04_21⁵¹, which contains global monthly emissions of NMVOC for eight sectors (Supplementary Table 2) between 1750 and 2019. Here we extracted gridded emissions data of NMVOC from CEDS during the period of 2000–2019. For individual VOC emissions, we calculated the scaling factors of 22 VOC species, including benzene, toluene, xylenes, big alkane (BIGALK: lumped $\geq C_4$ alkanes)^{47,52}, big alkene (BIGENE: lumped $\geq C_4$ alkenes)^{47,52}, acetylene, ethylene, ethanol, ethane, propylene, propane, formaldehyde, acet-aldehyde, acetone, methanol, formic acid, acetic acid, intermediate-VOC, semi-VOC, methyl ethyl ketone, acetonitrile, and hydrogen cyanide, based on the Coupled Model Intercomparison Project Phase 6 (CMIP6) inventory, which were then applied to scale the CEDS anthropogenic NMVOC emissions to estimate 22 VOC species' emissions between 2000 and 2019. We set intermediate-VOC emissions as 20% of NMVOC emissions and semi-VOC emissions as 60% of primary organic aerosol emissions⁵³. We also re-gridded CEDS NMVOC and 22 individual VOC emissions from their default 0.5° latitude by 0.5° longitude resolution to a 0.9° \times 1.25° latitude-longitude resolution, which is consistent with the CESM model resolution. Additionally, surface biomass burning emissions were based on the CMIP6 inventory developed by van Marle et al.⁵⁴.

To evaluate model performance in predicting surface NMVOC concentrations, we compared the modeled BTEX concentrations with in-situ observations from the US, Canada, and European countries where comprehensive VOC monitoring networks are available (Supplementary Discussion 1). Further details on CAM6-Chem model configuration and evaluation have been described explicitly on our previous study⁵ and elsewhere^{50,55,56}.

Health risk assessment

Our study involved the selection of 10 hazardous VOCs, namely formaldehyde, acetaldehyde, benzene, toluene, xylenes, propylene, methanol, methyl ethyl ketone, acetonitrile, and hydrogen cyanide, for health risk assessment based on their toxicity and carcinogenicity (see Supplementary Table 1). Before conducting the risk assessment, we calculated the population-weighted concentrations of each VOC, as shown in Eq. (1):

$$PWC_{i,j,k} = \frac{\sum (POP_{i,j} \times Conc_{i,j,k})}{\sum POP_{i,j}} \quad (1)$$

where $PWC_{i,j,k}$ refers to the population-weighted annual mean concentration of species (k) in the unit of $\mu\text{g m}^{-3}$ within grid box (i, j); $POP_{i,j}$ represents the population residing within each grid box (i, j). Data on global population count was downloaded from the NASA Socioeconomic Data and Application Center (SDAC) for the Gridded Population of the World, version 4 (GPWv4), with a horizontal resolution of 2.5 arc-minute⁵⁷. This data was further re-gridded to 0.1° latitude \times 0.1° longitude to facilitate country-wise analysis. $Conc_{i,j,k}$ represents the annual mean concentration of species (k) ($\mu\text{g m}^{-3}$) within the horizontal grid box (i, j), as determined by the CAM6-Chem monthly outputs.

We evaluated and detailed the chronic non-cancer risks associated with exposure to hazardous VOC in Supplementary Discussion 2. For cancer-associated risk assessment, we separately calculated it for specified age groups (from the third trimester to age 70, Supplementary Note 1) by accounting for greater susceptibility to carcinogens during early life exposure⁵⁸. The residential inhalation dose and lifetime inhalation cancer risk (LICR) of benzene, formaldehyde, and acetaldehyde for each age group are respectively estimated using Eqs. (2, 3):

$$Dose_{i,j,k,a} = PWC_{i,j,k} \times (BR/BW)_a \times EF \times 10^{-6} \quad (2)$$

$$LICR_{i,j,k,a} = Dose_{i,j,k,a} \times CPF_k \times ASF_a \times ED_a / AT \times FAR_a \quad (3)$$

where $Dose_{i,j,k,a}$ and $LICR_{i,j,k,a}$ refer to the residential inhalation dose ($\text{mg kg}^{-1} \text{d}^{-1}$) and lifetime inhalation cancer risk (unitless) of species (k) at each horizontal model grid box (i, j) for specified age group (a); $(BR/BW)_a$ denotes the breathing rate (BR) normalized to body weight (BW) in the unit of $\text{L kg}^{-1} \text{body weight d}^{-1}$ for each age group (a); EF is the exposure frequency (unitless); 10^{-6} is a unit conversion factor that converts micrograms to milligrams and liters to cubic meters; CPF_k is the inhalation cancer potency factor ($\text{mg} (\text{kg day})^{-1}$)⁻¹ of species (k); ASF_a , ED_a , and FAR_a are the age sensitivity factor (unitless), exposure duration (years), and the fraction of time spent at residential areas (unitless) for specified age group (a); and AT is the average time for lifetime cancer risk (years). The values of exposure variables used in the cancer risk estimation are listed in Supplementary Table 7. We calculated the excess lifetime cancer risk separately for each age group and carcinogen, then added them up to yield the integrated cancer risk at the receptor location. The risk estimated in this study are intended for the maximum exposed individual resident, using a health protective approach designed to prevent underestimation of public health impacts, especially during early life exposure. The uncertainty and 95% confidence interval of VOC-induced cancer risks were estimated based on the standard deviation of exposure parameter (BR/BW).

Apart from estimating individual non-cancer and cancer-associated risks, we also evaluated population-wide risk using the cancer burden method. This method takes into account the potential excess cancer cases that may occur in a population due to lifelong exposure to carcinogenic VOCs. It assumes a population (not necessarily the same individuals) will live in the impacted area for a lifetime (70 years). The cancer burden is calculated using Eqs. (4):

$$CB_{i,j,k} = LICR_{i,j,k} \times POP_{i,j} \quad (4)$$

where $CB_{i,j,k}$ and $LICR_{i,j,k}$ represent the cancer burden (CB) and LICR of species (k) for the grid box (i, j), respectively. We aggregated the total estimated number of potential cancers to determine the cancer burden at regional, national, and global scales. It is noteworthy that estimated cancer burden can be further translated into annual cancer cases by dividing the life expectancy in a specific country.

To provide a more comprehensive understanding of global health burdens associated with VOC exposure, we've followed the approach from our previous studies^{5,6,59} and divided the global into 11 regions: China, India, ROA, LATIN, SSA, ECEurope, NAME, the US, Canada, WEurope and ROW. The initial seven regions are classified as developing countries, while the latter four are considered developed, as per the International Monetary

Fund classification⁶⁰. This division allows for a detailed, multi-tiered discussion (scale: global-regional-country) of health burdens linked to different levels of VOC exposure.

Data availability

All data generated or analyzed during this study are included in this manuscript and its supplementary information files. The CEDS anthropogenic emission data used in this study are available at Zenodo (<https://doi.org/10.5281/zenodo.4741285>). CESM is an open-source community model and is publicly available at <https://github.com/ESCOMP/CESM> (last access: 8 August 2023).

Code availability

The codes for analysis, statistical computing and graphics are based on freeware environments, IDL (version 8.7.2, <https://www.nv5geospatialsoftware.com/Products/IDL>). All codes used in this study are available from the corresponding author upon request.

Received: 23 October 2023; Accepted: 15 February 2024;

Published online: 01 March 2024

References

1. Murray, C. J. et al. Global burden of 87 risk factors in 204 countries and territories, 1990–2019: a systematic analysis for the Global Burden of Disease Study 2019. *Lancet.* **396**, 1223–1249 (2020).
2. Jerrett, M. The death toll from air-pollution sources. *Nature* **525**, 330–331 (2015).
3. Pandey, A. et al. Health and economic impact of air pollution in the states of India: the Global Burden of Disease Study 2019. *Lancet Planet. Health* **5**, e25–e38 (2021).
4. McDuffie, E. E. et al. Source sector and fuel contributions to ambient PM_{2.5} and attributable mortality across multiple spatial scales. *Nat. Commun.* **12**, 3594 (2021).
5. Xiong, Y. et al. Long-term trends of impacts of global gasoline and diesel emissions on ambient PM_{2.5} and O₃ pollution and the related health burden for 2000–2015. *Environ. Res. Lett.* **17**, 104042 (2022).
6. Huang, Y., Partha, D. B., Harper, K. & Heyes, C. Impacts of global solid biofuel stove emissions on ambient air quality and human health. *GeoHealth* **5**, e2020GH000362 (2021).
7. Burnett, R. et al. Global estimates of mortality associated with long-term exposure to outdoor fine particulate matter. *Proc. Natl Acad. Sci.* **115**, 9592–9597 (2018).
8. Qiu, H. et al. Association of ambient non-methane hydrocarbons exposure with respiratory hospitalizations: a time series study in Taipei, Taiwan. *Sci. Total Environ.* **729**, 139010 (2020).
9. Ran, J. et al. Effects of ambient benzene and toluene on emergency COPD hospitalizations: a time series study in Hong Kong. *Sci. Total Environ.* **657**, 28–35 (2019).
10. Shah, A. S. et al. Global association of air pollution and heart failure: a systematic review and meta-analysis. *Lancet.* **382**, 1039–1048 (2013).
11. Shin, H. H. et al. Associations between personal exposures to VOCs and alterations in cardiovascular physiology: Detroit Exposure and Aerosol Research Study (DEARS). *Atmos. Environ.* **104**, 246–255 (2015).
12. Ma, C.-M. et al. Volatile organic compounds exposure and cardiovascular effects in hair salons. *Occup. Med. (Lond)* **60**, 624–630 (2010).
13. Choi, J. Y. et al. Ambient air pollution and the risk of neurological diseases in residential areas near multi-purposed industrial complexes of korea: A population-based cohort study. *Environ. Res.* **219**, 115058 (2023).
14. Cassidy-Bushrow, A. E. et al. Prenatal airshed pollutants and preterm birth in an observational birth cohort study in Detroit, Michigan, USA. *Environ. Res.* **189**, 109845 (2020).
15. *Integrated Risk Information System (IRIS) for Benzene and Formaldehyde.* (U.S. EPA, 2023); <https://www.epa.gov/iris>.
16. Strum, M. & Scheffe, R. National review of ambient air toxics observations. *J. Air Waste Manage. Assoc.* **66**, 120–133 (2016).
17. Xiong, Y., Bari, M. A., Xing, Z. & Du, K. Ambient volatile organic compounds (VOCs) in two coastal cities in western Canada: spatiotemporal variation, source apportionment, and health risk assessment. *Sci. Total Environ.* **706**, 135970 (2020).
18. Xiong, Y., Zhou, J., Xing, Z. & Du, K. Cancer risk assessment for exposure to hazardous volatile organic compounds in Calgary, Canada. *Chemosphere* **272**, 129650 (2021).
19. Xiong, Y., Huang, Y. & Du, K. Health risk-oriented source apportionment of hazardous volatile organic compounds in eight Canadian cities and implications for prioritizing mitigation strategies. *Environ. Sci. Tech.* **56**, 12077–12085 (2022).
20. Lerner, J. C., Sanchez, E. Y., Sambeth, J. E. & Porta, A. A. Characterization and health risk assessment of VOCs in occupational environments in Buenos Aires, Argentina. *Atmos. Environ.* **55**, 440–447 (2012).
21. Zhou, J. et al. Health risk assessment of personal inhalation exposure to volatile organic compounds in Tianjin, China. *Sci. Total Environ.* **409**, 452–459 (2011).
22. Xiong, Y. & Du, K. Source-resolved attribution of ground-level ozone formation potential from VOC emissions in Metropolitan Vancouver, BC. *Sci. Total Environ.* **721**, 137698 (2020).
23. Xiong, Y., Zhou, J., Xing, Z. & Du, K. Optimization of a volatile organic compound control strategy in an oil industry center in Canada by evaluating ozone and secondary organic aerosol formation potential. *Environ. Res.* **191**, 110217 (2020).
24. Galarneau, E. et al. Air toxics in Canada measured by the National Air Pollution Surveillance (NAPS) program and their relation to ambient air quality guidelines. *J. Air Waste Manage. Assoc.* **66**, 184–200 (2016).
25. Zhu, L. et al. Formaldehyde (HCHO) as a hazardous air pollutant: mapping surface air concentrations from satellite and inferring cancer risks in the United States. *Environ. Sci. Tech.* **51**, 5650–5657 (2017).
26. Partha, D. B., Cassidy-Bushrow, A. E. & Huang, Y. Global preterm births attributable to BTEX (benzene, toluene, ethylbenzene, and xylene) exposure. *Sci. Total Environ.* **838**, 156390 (2022).
27. Garcia-Gonzales, D. A., Shonkoff, S. B., Hays, J. & Jerrett, M. Hazardous air pollutants associated with upstream oil and natural gas development: a critical synthesis of current peer-reviewed literature. *Annu. Rev. Public Health* **40**, 283–304 (2019).
28. *Oil production in Alberta by year.* (Government of Alberta, 2023); <https://economicdashboard.alberta.ca/OilProduction>.
29. Bari, M. A. & Kindzierski, W. B. Ambient volatile organic compounds (VOCs) in Calgary, Alberta: sources and screening health risk assessment. *Sci. Total Environ.* **631–632**, 627–640 (2018).
30. Dimitriou, K. & Kassomenos, P. Background concentrations of benzene, potential long range transport influences and corresponding cancer risk in four cities of central Europe, in relation to air mass origination. *J. Environ. Manage.* **262**, 110374 (2020).
31. Hong, S.-H., Shin, D.-C., Lee, Y.-J., Kim, S.-H. & Lim, Y.-W. Health risk assessment of volatile organic compounds in urban areas. *Hum. Ecol. Risk Assess.* **23**, 1454–1465 (2017).
32. Hu, R., Liu, G., Zhang, H., Xue, H. & Wang, X. Levels, characteristics and health risk assessment of VOCs in different functional zones of Hefei. *Ecotoxicol. Environ. Saf.* **160**, 301–307 (2018).
33. Li, L. et al. Pollution characteristics and health risk assessment of benzene homologues in ambient air in the northeastern urban area of Beijing, China. *J. Environ. Sci.* **26**, 214–223 (2014).
34. Scott, P. S. et al. Observations of volatile organic and sulfur compounds in ambient air and health risk assessment near a paper mill in rural Idaho, U.S.A. *Atmos. Pollut. Res.* **11**, 1870–1881 (2020).
35. Tohid, L. et al. Spatiotemporal variation, ozone formation potential and health risk assessment of ambient air VOCs in an industrialized city in Iran. *Atmos. Pollut. Res.* **10**, 556–563 (2019).

36. Okada, Y. et al. Environmental risk assessment and concentration trend of atmospheric volatile organic compounds in Hyogo Prefecture, Japan. *Environ. Sci. Pollut. Res.* **19**, 201–213 (2012).

37. U.S. EPA. *Risk Assessment Guidance for Superfund: pt. A. Human health evaluation manual*. Vol. 1 (Office of Emergency and Remedial Response, US Environmental Protection Agency, 1989).

38. Health Canada. Federal contaminated site risk assessment in Canada: Guidance on Human Health Preliminary Quantitative Risk Assessment (PQRA) Version 3.0. (2021).

39. Graham, A. M. et al. Impact of the 2019/2020 Australian Megafires on Air Quality and Health. *GeoHealth*. **5**, e2021GH000454 (2021).

40. Both Angola and the Democratic Republic of the Congo Experiencing High Numbers of Agricultural Fires. (Jenner, L., 2020); <https://www.nasa.gov/image-feature/goddard/2020/both-angola-and-the-democratic-republic-of-the-congo-experiencing-high-numbers-of>.

41. Gilman, J. B., Lerner, B. M., Kuster, W. C. & De Gouw, J. Source signature of volatile organic compounds from oil and natural gas operations in northeastern Colorado. *Environ. Sci. Tech.* **47**, 1297–1305 (2013).

42. Edwards, P. M. et al. High winter ozone pollution from carbonyl photolysis in an oil and gas basin. *Nature* **514**, 351–354 (2014).

43. Zhu, L. et al. Long-term (2005–2014) trends in formaldehyde (HCHO) columns across North America as seen by the OMI satellite instrument: Evidence of changing emissions of volatile organic compounds. *Geophys. Res. Lett.* **44**, 7079–7086 (2017).

44. Country classifications by income levels (The World Bank, 2023); <https://datahelpdesk.worldbank.org/knowledgebase/articles/906519-world-bank-country-and-lending-groups>.

45. Mauderly, J. L. & Samet, J. M. Is there evidence for synergy among air pollutants in causing health effects? *Environ. Health Perspect.* **117**, 1–6 (2009).

46. Hoesly, R. M. et al. Historical (1750–2014) anthropogenic emissions of reactive gases and aerosols from the Community Emissions Data System (CEDS). *Geosci. Model Dev.* **11**, 369–408 (2018).

47. Emmons, L. K. et al. The Chemistry Mechanism in the Community Earth System Model Version 2 (CESM2). *J. Adv. Model. Earth Syst.* **12**, e2019MS001882 (2020).

48. Danabasoglu, G. et al. The community earth system model version 2 (CESM2). *J. Adv. Model. Earth Syst.* **12**, e2019MS001916 (2020).

49. Liu, X. et al. Description and evaluation of a new four-mode version of the Modal Aerosol Module (MAM4) within version 5.3 of the Community Atmosphere Model. *Geosci. Model Dev.* **9**, 505–522 (2016).

50. Tilmes, S. et al. Climate forcing and trends of organic aerosols in the Community Earth System Model (CESM2). *J. Adv. Model. Earth Syst.* **11**, 4323–4351 (2019).

51. O'Rourke P. R. S. et al. CEDS v_2021_04_21 Release Emission Data (v_2021_02_05) [Data set]. <https://doi.org/10.5281/zenodo.4741285> (2021).

52. Jo, D. S., Tilmes, S., Emmons, L. K., Wang, S. & Vitt, F. A new simplified parameterization of secondary organic aerosol in the community earth system model Version 2 (CESM2; CAM6.3). *Geosci. Model Dev.* **16**, 3893–3906 (2023).

53. Hodzic, A. et al. Rethinking the global secondary organic aerosol (SOA) budget: stronger production, faster removal, shorter lifetime. *Atmos. Chem. Phys.* **16**, 7917–7941 (2016).

54. Van Marle, M. J. et al. Historic global biomass burning emissions for CMIP6 (BB4CMIP) based on merging satellite observations with proxies and fire models (1750–2015). *Geosci. Model Dev.* **10**, 3329–3357 (2017).

55. Schwantes, R. H. et al. Evaluating the impact of chemical complexity and horizontal resolution on tropospheric ozone over the conterminous US with a global variable resolution chemistry model. *J. Adv. Model. Earth Syst.* **14**, e2021MS002889 (2022).

56. Vira, J., Hess, P., Ossouhou, M. & Galy-Lacaux, C. Evaluation of interactive and prescribed agricultural ammonia emissions for simulating atmospheric composition in CAM-chem. *Atmos. Chem. Phys.* **22**, 1883–1904 (2022).

57. Center for International Earth Science Information Network - CIESIN - Columbia University. *Gridded Population of the World, Version 4 (GPWv4): Population Count, Revision 11*, (2018).

58. California EPA. The air toxics hot spots program guidance manual for preparation of health risk assessments. (2015).

59. Huang, Y., Unger, N., Harper, K. & Heyes, C. Global climate and human health effects of the gasoline and diesel vehicle fleets. *GeoHealth*. **4**, e2019GH000240 (2020).

60. *World Economic and Financial Surveys World Economic Outlook Database-WEO Groups and Aggregates Information. (International Monetary Fund 2019)*; <https://www.imf.org/external/pubs/ft/weo/2020/01/weodata/groups.htm#oae>.

Acknowledgements

We greatly acknowledge high-performance computing support from the Cheyenne (doi:10.5065/D6RX99HX) provided by NCAR's Computational and Information Systems Laboratory. We also thank the Grid High Performance Computing (HPC) support from Wayne State University. Y. H. acknowledges support from the NSF (grant: AGS-2111428) and the Faculty Competition for Postdoctoral Fellows Program from the Office of Vice President for Research at Wayne State University. K. D. acknowledges support from the Canada Foundation for Innovation (grant: 35468).

Author contributions

Y.X. designed the study, performed model simulations and data analysis. Y.H. provided guidance on the CESM CAM6-Chem model simulations and acquired funding support. K.D. supervised health risk assessment of VOCs. Y.X. wrote the first draft of the paper and prepared the figures. All authors discussed the results and made substantial contributions to the final version of the paper.

Competing interests

The authors declare no competing interests.

Additional information

Supplementary information The online version contains Supplementary Material available at <https://doi.org/10.1038/s41612-024-00598-1>.

Correspondence and requests for materials should be addressed to Ying Xiong or Yaoxian Huang.

Reprints and permissions information is available at <http://www.nature.com/reprints>

Publisher's note Springer Nature remains neutral with regard to jurisdictional claims in published maps and institutional affiliations.

Open Access This article is licensed under a Creative Commons Attribution 4.0 International License, which permits use, sharing, adaptation, distribution and reproduction in any medium or format, as long as you give appropriate credit to the original author(s) and the source, provide a link to the Creative Commons licence, and indicate if changes were made. The images or other third party material in this article are included in the article's Creative Commons licence, unless indicated otherwise in a credit line to the material. If material is not included in the article's Creative Commons licence and your intended use is not permitted by statutory regulation or exceeds the permitted use, you will need to obtain permission directly from the copyright holder. To view a copy of this licence, visit <http://creativecommons.org/licenses/by/4.0/>.